*Journal of Chemical Crystallography, Vol. 29, No. 1, 1999*

# Crystal and molecular structure determination, TGA, DTA, and infrared and Raman spectra of rubidium nitroprusside monohydrate, $Rb_2[Fe(CN)_5NO]\cdot H_2O$

**D.B. Soria,[1] O.E. Piro,[2] E.E. Castellano,[3] and P.J. Aymonino[1]***

*Received September 16, 1997*

The crystal structure of rubidium nitroprusside monohydrate, $Rb_2[Fe(CN)_5NO] \cdot H_2O$, has been determined from X-ray diffraction data and refined using direct and Fourier methods to $R = 0.066$ and $Rw = 0.075$, employing 1894 independent reflections with $I > 3$ ($I$). The substance crystallizes in the monoclinic space group $C2/c$ ($C_{2h}^6$), with $a = 13.987(2)$, $b = 10.241(1)$, $c = 18.151(1)$ Å, $\beta = 110.94°$, and $Z = 8$. Anions are located at $C_1$ sites, one per asymmetric unit, and are slightly distorted octahedra. TGA, DTA, FTIR, and FTIR Raman results were interpreted on the basis of the formula of the compound, its crystal structure, and the behavior of other nitroprussides.

**KEY WORDS:** Rubidium nitroprusside monohydrate; crystal structure; properties.

## Introduction

As part of a thorough work on nitroprussides, which includes alkaline metal salts, we recently reported the crystal structure and thermal and vibrational behavior of anhydrous rubidium nitroprusside.[1] Now, we are making such a report for the monohydrated salt. This substance has been described by Gentil[2] and Tosi,[3] and in this latter case, together with a dihydrate. With the aim of solving the crystal structures of these hydrates and improving vibrational data, to compare results with those of the anhydrate (which can be directly crystallized from aqueous solutions), we attempted to obtain the hydrates, also from aqueous solutions, but have succeeded only with the monohydrate. Interest in these nitroprussides lie in the structural effects of hydration water, both on the ground and the metastable excited states (which we have studied by IR spectroscopy[4] and until recently believed to be electronic states, but now are suggested to be geometrical isomers[5]). The topotactical relationship which could exist between the hydrates and also, the anhydrate, were of interest as well. The anhydrate crystallizes in the orthorhombic, $P2_12_12_1$ ($D_2^4$, space group[1], while the monohydrate now reported belongs to the monoclinic, $C2/c$ ($C_{2h}^6$), group. There is no correlation between both structures.

[1] Centro de Química Inorgánica, (CEQUINOR) (CONICET, UNLP) and Laboratorio Nacional de Espectroscopía Óptica (LANAIS EFO) (CONICET-UNLP), Departamento de Química, Facultad de Ciencias Exactas, Universidad Nacional de La Plata, C.C., 9624, 1900 La Plata, R. Argentina.

[2] Programa PROFIMO (CONICET) and Laboratorio Nacional de Difracción de Rayos X (LANADI) (CONICET-UNLP), Departamento de Física, Facultad de Ciencias Exactas, Universidad Nacional de La Plata, C.C. 67, 1900 La Plata, R. Argentina.

[3] Instituto de Física de São Carlos, Universidade de São Paulo, C.P. 369, 13560 São Carlos (SP), Brazil.

* To whom correspondence should be adressed.

## Experimental

### *Preparative*

A solution of the compound was obtained by the common procedure of letting react silver nitroprusside and an aqueous solution of rubidium chlo-



1074-1542/99/0100-0075$16.00/0 

ride and evaporating the solvent to allow crystallization.[1] The crystals so obtained were redissolved in water and recrystallized by slowly evaporating the solvent at 30°C. Crystallization at a lower temperature (ca. 20°C) in a controlled atmosphere (over a saturated solution of sodium nitrite) and at the same temperature, but in open air, resulted in the formation of the monohydrate in both cases.

### *X-ray diffraction*

Small enough fragments of the crystals were used for X-ray diffraction. Crystal data, data collection procedure, and structure determination methods are summarized in Table 1.

### *TGA, DTA*

Thermal analyses were performed with Shimadzu TGA-50 and DTA-50H units, between room temperature and 500°C, at a heating rate of 5°C/min and nitrogen flow of 50 ml/min.

### *IR and Raman spectra*

The FTIR spectra were recorded with a Bruker IFS 113v spectrophotometer at 2 $cm^{-1}$ resolution and the Raman spectra with a Bruker IFS 66 instrument provided with the NIR Raman attachment, working at 4 $cm^{-1}$ resolution. A variable temperature Oxford OX8 ITL cell was used to run spectra of samples cooled with liquid air. The instruments were calibrated with atmospheric water and carbon dioxide bands and with sulphur, respectively.

## Results and discussion

### *Structural results*

Fractional coordinates and equivalent isotropic temperature parameters for $Rb_2[Fe(CN)_5NO] \cdot H_2O$ (RbNP) are given in Table 2. Bond distances and angles within the nitroprusside ion are included in Table 3. Figure 1 is an ORTEP[11] drawing of the compound showing the labelling of the atoms and their vibrational ellipsoids. The atomic anisotropic thermal parameters and the listing of observed and calculated structure factor amplitudes are provided as supple-

**Table 1.** Crystal Data, Data Collection Details and Structure Refinement Results for $Rb_2[Fe(CN)_5NO \cdot H_2O$

| | |
|---|---|
| Empirical formula | $C_5H_2FeN_6O_2Rb_2$ |
| CCDC deposit no. | CCDC-1003/5480 |
| Formula weight | 404.92 |
| Crystal color/shape | Red/paralellepiped |
| Temperature | 293(2) K |
| Crystal system | Monoclinic |
| Space group | $C2/c$ |
| Unit cell dimensions[a] | |
| $a$ = 13.987(3) Å | |
| $b$ = 10.241(2) Å | |
| $c$ = 18.151(3) Å | |
| $\beta$ = 110.94(2)° | |
| Volume | 2428.3(8) $Å^3$ |
| $Z$ | 8 |
| Density (calculated) | 2.215 $Mg/m^3$ |
| Absorption coefficient | 9.202 $mm^{-1}$ |
| Crystal size | 0.1 × 0.15 × 0.2 mm |
| Diffractometer/scan | Enraf-Nonius CAD-4/$\omega$-2$\theta$ |
| Radiation, graphite monochr. | Mo$K\alpha$, $\lambda$ = 0.71069 Å |
| $\theta$ range for data collection | 2.40 to 24.97° |
| Index ranges | $-16 \le h \le 15$, $0 \le k \le 12$, $0 \le 1 \le 21$ |
| Reflections collected | 2346 |
| Independent reflections | 1894 [R(int) = 0.022] |
| Observed reflections [$I > 2\sigma(I)$] | 1343 |
| Data reduction and correction[b] | SDP[7], SHELX-76[8], |
| Structure solution and refinement[c] programs | SHELX-86[9], SHELX-93[10] |
| Refinement method | Full-matrix least-squares on $F^2$ |
| Weights, $w$ | $w = [\sigma^2(F_o^2) + (0.0389P)^2]^{-1}$ with $P = [\mathrm{Max}(F_o^2, 0) + 2F_c^2]/3$ |
| Data/restraints/parameters | 1894/0/146 |
| Goodness-of-fit on $F^2$ | 1.017 |
| Final $R$ indices [$I > 2$sigma($I$)] | $R1$ = 0.032, $wR2$ = 0.064 |
| $R$ indices (all data) | $R1$ = 0.066, $wR2$ = 0.075 |
| Largest diff. peak and hole | 0.56 and −0.51 e.$Å^{-3}$ |

[a] Least-squares refinement of $[(\sin\theta)/\lambda]^2$ values for 24 reflections in the $19.78 < 2\theta < 33.34°$ range.
[b] Correctons: Lorentz, polarization and absorption[6] (min. and max. transmission factors were 0.483 and 0.634).
[c] Structure solved by Patterson and Fourier methods and the final molecular model obtained by anisotropic full-matrix least-squares refinement for the non-H-atoms employing neutral scattering factors and anomalous dispersion corrections. The water hydrogen atoms were located in a difference Fourier map. They were included fixed in the molecular model with a common isotropic thermal parameter.

**Table 2.** Fractional Atomic Coordinates ($\times 10^4$) and Isotropic Temperature Factors ($Å^2 \times 10^3$) for $Rb_2[Fe(CN)_5NO] \cdot H_2O$[a]

| Atom | *X*/*a* | *Y*/*b* | *Z*/*c* | *U*(eq) |
|---|---|---|---|---|
| Rb(1) | 10375(1) | 1066(1) | 6254(1) | 35(1) |
| Rb(2) | 6658(1) | 831(1) | 3410(1) | 40(1) |
| Fe | 6997(1) | −528(1) | 5709(1) | 22(1) |
| N | 6191(3) | −1354(4) | 4960(3) | 26(1) |
| O | 5648(3) | −1848(4) | 4411(3) | 46(1) |
| C(1) | 8035(4) | −473(5) | 5233(3) | 25(1) |
| N(1) | 8630(4) | −448(5) | 4941(3) | 36(1) |
| C(2) | 6111(4) | −496(6) | 6322(3) | 28(1) |
| N(2) | 5573(4) | −562(6) | 6667(3) | 47(2) |
| C(3) | 7971(5) | 523(6) | 6525(3) | 26(1) |
| N(3) | 8558(4) | 1183(5) | 6975(3) | 40(1) |
| C(4) | 7658(4) | −2043(6) | 6339(4) | 30(1) |
| N(4) | 8011(5) | −2937(5) | 6706(3) | 49(2) |
| C(5) | 6464(4) | 1145(6) | 5240(3) | 27(1) |
| N(5) | 6129(4) | 2106(5) | 4949(3) | 44(1) |
| Ow | 8679(4) | 1537(5) | 3372(3) | 56(1) |
| H(1) | 8740 | 1958 | 3791 | 85(22) |
| H(2) | 8747 | 1983 | 3006 | 85(22) |

[a] *U*(eq) is defined as one third of the trace of the orthogonalized *Uij* tensor.

**Table 3.** Intramolecular Bond Distances (Å) and Angles (°) in the Nitroprusside Ion

| | |
|---|---|
| Bond distances | |
| Fe−N | 1.655(5) |
| Fe−C(1) | 1.938(6) |
| Fe−C(2) | 1.938(6) |
| Fe−C(3) | 1.940(6) |
| Fe−C(5) | 1.941(6) |
| Fe−C(4) | 1.952(6) |
| N−O | 1.135(6) |
| C(1)−N(1) | 1.136(6) |
| C(2)−N(2) | 1.140(7) |
| C(3)−N(3) | 1.148(7) |
| C(4)−N(4) | 1.136(7) |
| C(5)−N(5) | 1.136(7) |
| Bond angles | |
| N−Fe−C(1) | 92.7(2) |
| N−Fe−C(2) | 95.3(2) |
| N−Fe−C(3) | 175.3(2) |
| N−Fe−C(4) | 96.7(2) |
| N−Fe−C(5) | 92.7(2) |
| C(1)−Fe−C(2) | 171.8(2) |
| C(1)−Fe−C(3) | 83.8(2) |
| C(1)−Fe−C(4) | 90.6(2) |
| C(1)−Fe−C(5) | 90.5(2) |
| C(2)−Fe−C(3) | 88.4(2) |
| C(2)−Fe−C(4) | 86.8(2) |
| C(2)−Fe−C(5) | 90.7(2) |
| C(3)−Fe−C(4) | 86.4(2) |
| C(3)−Fe−C(5) | 84.3(2) |
| C(4)−Fe−C(5) | 170.5(2) |
| Fe−N−O | 174.8(5) |
| Fe−C(1)−N(1) | 178.8(5) |
| Fe−C(2)−N(2) | 175.4(6) |
| Fe−C(3)−N(3) | 176.1(5) |
| Fe−C(4)−N(4) | 177.7(6) |
| Fe−C(5)−N(5) | 178.1(5) |

mentary material. Anions have the expected pseudo-octahedral structure, with the equatorial CN groups slightly bent towards the axial (opposite to NO) CN group and the NCFeNO axis slightly bent. The anions lie at $C_1$ sites (ideal symmetry: $C_{4v}$). Figure 2 shows a view of the unit cell and Figure 3 presents in detail the alternate, antiparallel, disposition of anions along rows. Distance between neighbors is 4.34 Å. Water molecules lie also at $C_1$ sites.

## *TGA, DTA*

Thermograms of RbNP show that the dehydration process begins at a relatively low temperature, producing a DTA peak located at 67°C. The weight loss in this endothermic step corresponds very closely to one water molecule per formula weight (theoretical: 4.5%, measured: 4.3%, as mean value of two typical runs).

The following decomposition steps are observed as two closely located endothermic peaks at 290 and 315°C, the first involving perhaps the loss of NO, followed by 1/2 $C_2N_2$ in the second peak, as it happens with other nitroprussides[12] and in the anhydrous compound.[1] The weight change observed as a result of these two processes was 13.4% in two runs (expected: 13.4%). A third DTA peak at 402°C is probably due

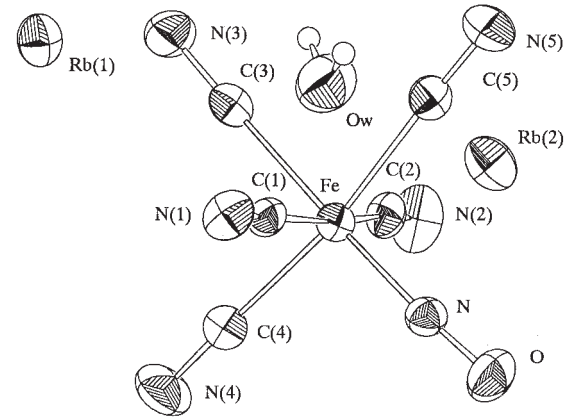


**Fig. 1.** ORTEP drawing of $Rb_2[Fe(CN)_5NO] \cdot H_2O$. Vibrational ellipsoids correspond to 50% probability.

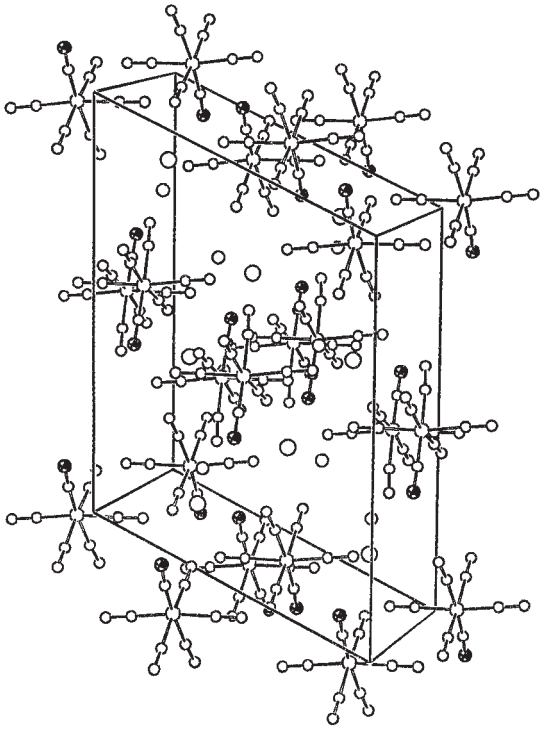

**Fig. 2.** ORTEP projection of $Rb_2[Fe(CN)_5NO] \cdot H_2O$. Nitrosyl oxygens are identified by circles with crosses.

to an exothermic phase transition because it was not accompanied by a weight change. It is interesting to note that the same process occurs in the case of potassium nitroprusside sesquiquarterhydrate, $K_2[Fe(CN)_5NO] \cdot 1.25H_2O$.[13]

*IR and Raman spectra*

The IR spectra of RbNP were recorded at room and low temperature (ca. 80 K). The main features of the spectra can be immediately assigned to the internal vibrations of the hydration water molecule and the nitroprusside anion. The Raman spectrum was recorded at room temperature. Wavenumbers of the IR absorption and Raman scattering bands due to the anion and their tentative assignments are reported in Table 4. As in the anhydrous compound,[1] there is only one crystallographic type of anion in RbNP located at $C^5$ sites, which are slightly distorted from ideal $C_{4v}$ symmetry. Therefore, the assignments

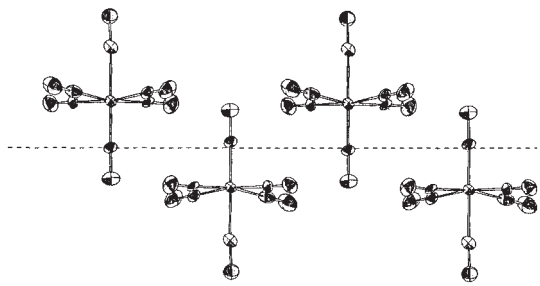

**Fig. 3.** Dispositions of anions in $Rb_2[Fe(CN)_5NO] \cdot H_2O$ along rows.

**Table 4.** Observed Raman and IR Bands and Assignments for the Anion in $Rb_2[Fe(CN)_5NO] \cdot H_2O$[a]

| Symmetry species under $C_4v$ | Raman(r.t.) | FTIR(r.t) | FTIR(l.t) | Assignment |
|---|---|---|---|---|
| | | 3850(vw) | 3855(w) | $2\nu$NO |
| $A_1$ | 2153(vs) | 2154(sh) | 2156(vw) | $\nu$CNax |
| $A_1$ | 2148(sh) | 2148(m) | 2151(m) | $\nu$CN |
| $B_1$ | | 2143(vs) | $\nu$CN | |
| E | 2138(sh) | 2139(vs) | 2140(vs) | $\nu$CN |
| | | 2111(vw) | 2114(vw) | $\nu^{12}C^{15}N$ |
| | | 2099(vw) | 2102(vw) | $\nu^{13}C^{14}N$ |
| | | 2095(vw) | 2097(vw) | $\nu^{13}C^{14}N$ |
| $A_1$ | 1942(vw) | 1956(sh) | 1960(vs) | $\nu$NO |
| $A_1$ | 1926(vw) | 1949(vs) | 1952(vs) | $\nu$NO |
| | | 1928(sh) | 1932(sh) | ? |
| | | 1921(m) | 1922(m) | $\nu^{15}N^{16}O$ |
| | | 1899(vw) | 1900(vw) | ? |
| | | 1896(sh) | 1896(vw) | ? |
| E | 662(vw) | 662(w) | 665(w) | $\delta$FeNO |
| E | | 656(m) | 659(m) | $\delta$FeNO |
| $A_1$ | 647(vw) | 648(vw) | 650(vw) | $\nu$FeN |
| E | 503(vw) | 502(m) | 505(m) | $\delta FeCN_{ax}$ |
| $A_1$ | 462(vw) | 457(w) | 460(w) | $\nu FeC_{ax}$ |
| E | | 429(w) | 432(w) | $\nu$FeC |
| | 422(vw) | 416(s) | 418(s) | $\nu$FeC |
| | 408(vw) | 409(s) | 412(s) | $\nu$FeC |
| | 393(w) | 390(w) | 393(w) | $\nu$FeC |
| | | | 374(w) | $\nu$FeC |
| | | 325(vw) | 326(vw) | $\delta$FeCN |
| | | 321(vw) | 322(vw) | $\delta$FeCN |
| | | 215(vw) | 216(vw) | ? |
| | 166(m) | | | l.m. |
| | 146(sh) | | | $\delta$CFeN |
| | 136(m) | | | l.m. |
| | 119(sh) | | | $\delta$CFeN |
| | 98(sh) | | | $\delta FeC_{ax}$ |
| | 86(vw) | | | $\delta$CFeC + $\delta$CFeN |
| | ca.73(vw) | | | l.m. |
| | ca.60(vw) | | | l.m. |

[a] Wavenumbers in $cm^{-1}$; vs: very strong, s: strong, m: medium, w: weak, vw: very weak, sh: shoulder, l.m.: lattice mode. Note: C and C-bonded N atoms are equatorial unless otherwise stated.

will be mainly based on this group, but in some cases a lower real symmetry will be considered.

The assignments of bands due to the nitroprusside anion are as follows.

*CN stretching bands*

Three features are observed in the room temperature IR spectrum, at 2154 (sh), 2148 (m) and 2139 (vs) $cm^{-1}$. These features do not differ significantly in wavenumbers from corresponding features in the anhydrous compound.[1] In the low temperature IR spectrum four bands at 2156 (vw), 2151 (m), 2143 (vs), and 2140 (vs) $cm^{-1}$ are seen. In the Raman spectrum only one band appears at 2153 $cm^{-1}$. These bands are due to the most abundant $^{12}C^{14}N$ groups. The band at 2153 $cm^{-1}$ (IR, R) is assigned to the $A_1$ (axial) mode, in comparison with the anhydrous salt. The IR bands at 2148 (r.t.) and 2151 (l.t.) should correspond to the $A_1$ (equatorial) mode. In the low temperature spectrum, the band at 2143 $cm^{-1}$ is assigned to the $B_1$ (eq) mode by comparison with the anhydrous compound and the very strong band at 2140 $cm^{-1}$, to the E(eq) mode. The very weak feature located at 2111 $cm^{-1}$ in the room temperature IR spectrum, which shifts to 2114 $cm^{-1}$ at low temperature, is perhaps due to the most abundant, equatorial, isolated, isotopic $^{12}C^{15}N$ groups, because in the room temperature spectrum of the anhydrous compound it appears as a shoulder at 2110 $cm^{-1}$. Isolated $^{13}C^{14}N$ (eq) groups give place perhaps to the features at 2102 and 2097 $cm^{-1}$ (l.t.), because in $^{13}C$-labelled nitroprusside spectrum similar features appear at 2109.7 and 2098.1 $cm^{-1}$.[14] As in this latter case, the splitting of bands seems to confirm the symmetry of the anion lower than $C_{4v}$, although only two of the four expected bands for $C_1$ seem to be observed.

*NO and FeNO vibrational bands*

Two features are seen in the IR room temperature spectrum in the NO fundamental stretching region, at 1956 and 1949 $cm^{-1}$, as expected from factor group splitting (Au, Bu under factor group $C_{2h}$ symmetry). In the low temperature spectrum these two features shift to 1960 and 1956 $cm^{-1}$, respectively, and the first of them shows up more clearly than at room temperature. In the Raman spectrum, as result of the accumulation of 2000 runs, two very weak features, merging distinctly enough from the noise level at 1942 and 1927 $cm^{-1}$ (the first weaker than the second) should be assigned to the weak dispersing polar NO groups. These two features should be the expected counterparts (Ag, Bg) of the IR bands under $C_{2h}$ factor group symmetry. Mean values of the IR and Raman room temperature $\nu$NO wavenumbers, 1952.5 and 1934.5 $cm^{-1}$, differ as much as 18 $cm^{-1}$. This strong Davydov splitting is due to the vibrational dipole–dipole coupling between neighboring antiparallel NO groups. In $Ba[Fe(CN)_5\ NO] \cdot 3H_2O$ the difference amounts 11 $cm^{-1}$ [15,16] and in $Mn[Fe(CN)_5NO] \cdot 2H_2O$, 10 $cm^{-1}$.[17]

The apparently medium intense band (strengthened by the partial superposition with one of the very strong stretching bands of isotopically normal NO) observed in the room temperature IR spectrum at 1921 $cm^{-1}$, is assigned to the isotopic species $^{15}N^{16}O$ (natural abundance 0.38%) (expected from the mean value 1952.5 $cm^{-1}$: 1921 $cm^{-1}$, as calculated with a diatomic model). There is no feature to be assigned to the less abundant (0.20%)$^{14}N^{18}O$ groups (expected at 1915 $cm^{-1}$). For $^{15}N^{18}O$ groups, due to very low natural abundance, no visible feature could be expected.

IR bands at 662 and 656 $cm^{-1}$ (r.t.) and at 665 and 659 $cm^{-1}$ (l.t.) are assigned to the partially splitted FeNO bending mode, which in the Raman spectrum appears as a single band at 662 $cm^{-1}$. The FeN stretching is assigned to the room temperature IR and Raman single features (no splitting is observed) located at 648 $cm^{-1}$ (650 $cm^{-1}$ at l.t.) and 647 $cm^{-1}$, respectively.

*FeC stretchings and FeCN deformations*

The assignments of bands supposedly due to these modes (Table 4) were made following reference 14.

*CFeC and CFeN deformations*

Several bands due to these anion modes appear below 150 $cm^{-1}$ (c.f. reference 14 and were observed only in the Raman spectra. Assignments also follow reference 14.

Wavenumbers from the low temperature IR spectra are used in the following discussion of bands due to water.

The two bands located at 3606 and 3513 $cm^{-1}$, respectively, are assigned to the antisymmetric and

symmetric stretching modes, respectively. The single band appearing at 1608 $cm^{-1}$ is assigned to the bending mode. The existence of no more than three bands in these regions confirm the presence of only one type of hydration water.

The librational bands appear between 790 and 300 $cm^{-1}$ in the IR spectra of other nitroprussides, often overlapped with bands of the anion[14] (and references therein). The hipsochromic shift, the increase in intensity, and the decrease in half–widths upon cooling are typical for bands due to the external vibrations of water. On this basis, the features observed at 495, 392, and 379 $cm^{-1}$ are assigned to librational modes. The assignment of these features to twisting or torsion around an axis bisecting the water molecule (T), out–of–plane wagging (W), and in–plane rocking (R) is, in general, difficult. The torsion should not be active if the water molecules are symmetric but, being asymmetric ($C_1$), some degree of mixing between the librational modes should occur and the torsion should become active. By comparison with assignments proposed for $Cs_2[Fe(CN)_5NO] \cdot H_2O$,[18] (CsNP) the sequence $\nu_T > \nu_W > \nu_R$ is adopted. So, the bands at 494, 392, and 379 are assigned to the twisting, wagging, and rocking modes, respectively. It is to be noted that in CsNP[18] the bands' wavenumbers are higher than in the present case, probably due to the lower symmetry of the water molecule as reflected by the difference between $\nu_1$ and $\nu_3$, 191 $cm^{-1}$ in the CsNP and 93 $cm^{-1}$ in RbNP.

## Acknowledgments

We thank FINEP, FAPESP and Fundação Vitae of Brazil (E.E.C.), CONICET, R. Argentina (CEQUINOR and PROFIMO) and CICPBA (CEQUINOR) for financial support. The spectroscopic work was performed at the National Laboratory for Research and Services in Optical Spectrophotometry (LANAIS EFO), La Plata, R. Argentina. Part of the X-ray diffraction experiments were carried out at the National Diffraction Laboratory (LANADI), La Plata, R. Argentina.

## References

1. Soria, D.B.; Amalvy, J.I.; Piro, O.E.; Castellano, E.E.; Aymonino, P.J. *J. Chem. Crystallogr.* **1996**, *26,* 315.
2. Gentil, L.A. *Doctoral Thesis,* Facultad de Ciencias Exactas, Universidad Nacional de La Plata, R. Argentina, 1973.
3. Tosi, L. *Compt. Rend.* **1973**, *277C,* 335.
4. Güida, J.A.; Aymonino, P.J.; Piro, O.E.; Castellano, E.E. *Spectrochim. Acta* **1993**, *49A,* 535.
5. Fomitichev, D.V.; Coppens, P. *Inorg. Chem.* **1996**, *35,* 7021.
6. Busing, W.R.; Levy, H.A. *Acta Crystallogr.* **1957**, *10,* 180.
7. Frenz, B.A. *Enraf-Nonius Structure Determination Package;* Enraf-Nonius: Delft, The Netherlands, 1983.
8. Sheldrik, G.M. *SHELXL-76. A Program for Crystal Structure Determination;* University of Cambridge: England, 1976.
9. Sheldrik, G.M. *Acta Crystallogr.* **1990**, *A46,* 467.
10. Sheldrik, G.M. *SHELXL-93. A Program for Crystal Structure Refinement*; University of Götingen: Germany, 1993.
11. Johnson, C.K. *ORTEP. Report ORNL-3794;* Oak Ridge; TN:USA, 1965.
12. Zuriaga, M.J.; Monti, G.A.; Martin, C.A.; Güida, J.A; Piro, O.E.; Aymonino, P.J.; Sala, O. *J. Thermal Anal.* **1991**, *37,* 1523.
13. Amalvy, J.I.; Varetti, E.L.; Castellano, E.E.; Piro, O.E.; Punte, G.; Aymonino, P.J. *J. Cryst. Spectrosc. Res.* **1986**, *16,* 537.
14. Chacón Villalba, M.E.; Varetti, E.L.; Aymonino, P.J. *Vibrat. Spectrosc.* **1992,** *4,* 109; Chacón Villalba, M.E.; Varetti, E.L.; Aymonino, P.J. *Vibrat. Spectrosc.* **1997**, *14,* 275.
15. González, S.R.; Aymonino, P.J.; Piro, O.E. *J. Chem. Phys.* **1984,** *81,* 625; González, S.R.; Piro, O.E.; Aymonino, P.J.; Castellano, E.E. *Phys. Rev. B15* **1986**, *33,* 5814.
16. Güida, J.A.; Piro, O.E.; Aymonino, P.J.; Sala, O. *J. Raman Spectrosc.* **1992**, *23,* 131.
17. Benavente, A.; Morán, J.A. de; Piro, O.E.; Castellano, E.E.; Aymonino, P.J. *J. Chem. Crystallogr*. **1997,** *27,* 343.
18. Vergara, M.; Varetti E.L. *J. Phys. Chem. Solids* **1987**, *48,* 13.